Chemical bonding and electronic properties of SeS_2-treated GaAs(100)

Jingxi Sun,[a] Dong Ju Seo,[b] W. L. O'Brien,[c] F. J. Himpsel,[b] A. B. Ellis,[d] and T. F. Kuech[a]
University of Wisconsin-Madison, 1415 Engineering Drive, Madison, Wisconsin 53706

(Received 7 November 1997; accepted for publication 16 October 1998)

SeS_2-passivated *n*-type GaAs (100) surfaces, formed by treatment of GaAs in SeS_2:CS_2 solution at room temperature, were studied with high-resolution core-level photoemission spectroscopy excited with synchrotron radiation source. The SeS_2-treated surface consists of a chemically stratified structure of several atomic layers thickness. Arsenic-based sulfides and selenides reside in the outermost surface layer while gallium-based selenides are adjacent to the bulk GaAs substrate. The shift of the surface Fermi level within the band gap was monitored during controlled thermal annealing, allowing for the identification of the specific chemical entities responsible for the reduction in surface band bending. Arsenic-based species are removed at low annealing temperature with little shift of the Fermi level. Gallium-based selenides are shown to be associated with the unpinning of the surface Fermi level. © *1999 American Institute of Physics.*
[S0021-8979(99)06602-5]

I. INTRODUCTION

Compound semiconductors, such as GaAs and InP, are widely used for high-speed semiconductor devices as well as other microelectronic and optoelectronic devices. Most III–V compound semiconductors, particularly GaAs, possess a high density of midgap surface states that have slowed the development of many potential applications. The stable passivation of the GaAs surface continues to be a problem in the development of GaAs-based technology.

The passivation of a semiconductor is defined as the elimination or severe reduction in the chemical and electrical reactivity at either an interface/surface or throughout its bulk.[1] The passivation of a semiconductor generally involves the modification of the properties of ''dangling'' or reactive bonds. The passivation of the semiconductor by the removal of midgap states is related to chemical changes within the material.[1] The chemical bonding at the surface after passivation will determine the surface electronic properties.

There has been a great deal of research on the passivation of the surface and interface states in the GaAs-based structures. The approaches to GaAs surface passivation include the epitaxial growth of heterostructures,[2,3] plasma treatment,[4–6] and chemical treatment.[7–9] These techniques can reduce the density and impact of surface states on certain device properties. The impact of a particular passivation procedure is often noted through enhanced photoluminescence (PL) intensity from the passivated semiconductor. The enhanced PL intensity has been attributed to both a reduction in the surface state density and the reduced surface recombination velocity. The specific impact of the surface electronic structure remains of continuing interest.

Chalcogen atoms (S, Se, and Te) have been found to be useful passivating agents for GaAs surfaces.[10,11] The treatments of GaAs surfaces by sulfide-containing solutions have been shown to produce a strong increase of the PL intensity in a variety of studies.[12–14] Although this method improves the surface electronic properties of GaAs(100), the long-term stability of these aqueous-based sulfide passivation techniques is often very poor. Anodic sulfurized GaAs has been shown to be more resilient to long-term degradation than previous aqueous-based approaches.[15,16] Other group VI elements, such as Se or Te, may provide a more stable passivation. Elemental Se can easily incorporate into the surface giving rise to a Ga–Se phase.[17] The most stable phase is found to be Ga_2Se_3, which has a close lattice match to GaAs, forming a layer with very little strain on the GaAs surface,[18] A lattice-matched passivating layer can reduce the density of the midgap states attributable to surface structure disorder. The Se-treated surfaces have been demonstrated to be more stable over time than S-treated surfaces.[9] A stable Se-based passivation layer can be produced on the GaAs(100) surface by contact with a SeS_2 solution.[19–22] This treatment appears to be very effective in forming Se-based species on GaAs surface and in improving the electronic properties through the formation of a thermally and chemically stable passivating layer.[2] As in many other cases of chemical-based surface passivation, the underlying passivating mechanism of the SeS_2-treated GaAs(100) surface still is not clearly understood. Knowledge of the surface reactions induced by the SeS_2-based treatment, the chemical bonding at the treated surfaces and the corresponding electronic properties is presently incomplete and is addressed in this study.

A general relationship between the surface electronic properties and the chemical bonding at GaAs(100) surfaces has not been established since this relationship may be unique to the chemical system employed. In order to develop models of chemical-based passivation on the III–V semiconductor surfaces, detailed measurements of the chemical

[a]Department of Chemical Engineering; electronic mail: sunj@amps.che.wisc.edu
[b]Department of Physics.
[c]Synchrotron Radiation Center.
[d]Department of Chemistry.

 © 1999 American Institute of Physics

Downloaded 29 Dec 2006 to 128.104.198.71. Redistribution subject to AIP license or copyright, see http://jap.aip.org/jap/copyright.jsp

bonding and Fermi level position on the passivated surface have been undertaken for III–V semiconductors.[23–25] In this article, the GaAs(100) surfaces passivated by SeS_2, using wet chemical techniques, have been studied in detail with high-resolution, core-level photoemission spectroscopy excited with synchrotron radiation source. Core-level spectra exhibiting predominantly either surface or bulk features have been obtained using the tunability of synchrotron radiation source. These results reveal a rich surface-derived substructure that is due to changes in the near-surface chemical bonding environment. The core-level shifts induced by surface Fermi level movements have been identified. A structural layer model, which is indicative of the surface reactions leading to surface passivation, is proposed based on the analysis of the spectroscopic results. The correlation between the electronic properties of the GaAs surface and the chemical bonding on this surface will be presented.

II. EXPERIMENTAL PROCEDURES

The native oxide on the surface was initially removed with HCl:H_2O (1:1) solution and blown dry with N_2 gas. The samples were subsequently dipped into a saturated solution of SeS_2 in CS_2 for ~40 s. Any excess SeS_2 on the surface was removed by repeated CS_2 rinsing. The above treatment was performed at room temperature. Samples prepared using above described SeS_2 treatment will be referred to as the "as-treated" samples. "HCl-cleaned-only" samples that were not subsequently treated by SeS_2 were used as a reference. The effect of SeS_2 treatment on the electronic properties of the surface was investigated by PL. The PL measurements were carried out at 295 K using an argon ion laser as the source of excitation with an illumination power density of $\sim 15\ \mathrm{W/cm^2}$. PL measurements were performed on both n- (Si-doped $\sim 5\times 10^{16}\ \mathrm{cm^{-3}}$) and p- (C-doped $\sim 5\times 10^{15}\ \mathrm{cm^{-3}}$) GaAs(100). The photoemission experiments were carried out at the Synchrotron Radiation Center (SRC) of the University of Wisconsin-Madison. Si-doped n-type GaAs(100), with a carrier density of $1\times 10^{18}\ \mathrm{cm^{-3}}$, was used in photoemission studies. The samples were placed in a vacuum desiccator for storage and transfer. The desiccator has been used in order to minimize the influence of surface contamination, e.g., hydrocarbon from the air, on the subsequent photoemission results. All samples were exposed to the room ambient during mounting and transfer to the photoemission chamber. Monochromatic light of different photon energies was used to control the emitted electron kinetic energy to enable the depth profiling. The photoelectrons were analyzed with a double pass cylindrical mirror electron kinetic energy analyzer (CMA). Kinetic energies (KE) of 40 and 300 eV, corresponding to photoelectron escape depths of ~0.5 and 1.5 nm, were utilized. These specific values of KE were used to measure the surface-sensitive and bulk-sensitive spectra, respectively. A clean GaAs(100) surface, free of oxides, was obtained by thermal annealing up to 600 °C in the photoemission chamber under ultrahigh vacuum (UHV). This thermal-cleaned surface was used as a reference for subsequent measurements. The Fermi level position on the sample holder was determined relative to a reference sample of Ta foil that was cleaned by argon sputtering and thermal annealing. In order to investigate the nature of chemical bonding on the surface, the as-treated samples were annealed for ~10 min in the photoemission chamber under UHV at increasing temperatures. The sample temperature during thermal annealing was measured by an optical pyrometry.

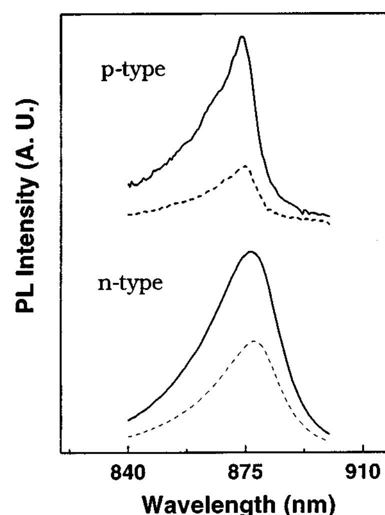

FIG. 1. Photoluminescence response from the SeS_2 as-treated (solid) and HCl-cleaned-only (dash) GaAs surfaces. The photoluminescence intensity was increased after SeS_2 treatment for both n- and p-GaAs(100).

III. RESULTS

The results will be divided along the two classes of measurements obtained in this study. The results of the measurements used to determine the properties of the as-treated surface are presented in the first section. Results of thermal annealing experiment are then presented in order to determine the relationship between specific species on the surface and the surface Fermi level position.

A. Studies of the as-treated surface

1. Photoluminescence study

Figure 1 shows the room-temperature PL spectra of the SeS_2 as-treated and HCl-cleaned-only samples for both n- and p-GaAs(100). The SeS_2 as-treated and HCl-cleaned-only samples are of same piece of GaAs. The PL intensity was increased by a factor of 2–5 after SeS_2 treatment on both n- and p-type samples. This PL intensity enhancement is repeatable. These spectra indicate that the SeS_2 treatment results in the flattening of the bands near the surface, due to the motion of the surface Fermi level position, or a reduction in the surface recombination velocity.

2. Core-level photoemission intensity ratios and stoichiometry

The surface chemistry and stoichiometry of the as-treated surface were systematically studied by measuring the relative peak intensity ratios between As 3d, Ga 3d, Se 3d, and S 2p core-level photoemission spectra. The changes of photoemission peak intensity ratios between the different el-

Downloaded 29 Dec 2006 to 128.104.198.71. Redistribution subject to AIP license or copyright, see http://jap.aip.org/jap/copyright.jsp

TABLE I. Atomic concentration ratios of As-to-Ga, Ga-to-Se, and Se-to-S for SeS_2 as-treated and HCl-cleaned-only GaAs(100) surfaces. Kinetic energies (KE) of 40 and 300 eV, corresponding photoelectron escape depth of ~0.5 and 1.5 nm, were utilized. These specific values of KE were used to measure the surface-sensitive and bulk-sensitive spectra, respectively.

SeS_2 as-treated GaAs(100)			
	As/Ga	Ga/Se	Se/S
Surface-sensitive	2.5±0.1	1.9±0.1	1.3±0.1
Bulk-sensitive	1.9±0.1	3.7±0.1	1.7±0.1
HCl-cleaned-only GaAs(100)			
Surface-sensitive	0.9±0.1	⋯	⋯
Bulk-sensitive	1.0±0.1	⋯	⋯

ements with excitation wavelength were used to deduce the in-depth elemental composition resulting from the SeS_2 treatment.

The peak intensity ratios were evaluated from spectra taken at a low instrumental resolution in order to achieve a higher measurement signal. Diffraction effects in the measured intensities should be small due to the angularly integrated spectra taken with the CMA. Both surface-sensitive and bulk-sensitive measurements were performed by varying the incident photon energy. The atomic concentration ratios can be approximately determined from the photoemission peak intensity ratio using corrections for both photoionization cross section and the transmission function of the spectrometer. The atomic concentration ratio is given by

$$\frac{C_i}{C_j}=\frac{I_i}{I_j}\times\frac{\sigma_j}{\sigma_i}\times\frac{T_j}{T_i}, \tag{1}$$

where C_i is the atomic concentration, I_i is the intensity of the core-level photoemission peak, σ_i is the photoionization cross section, T_i is the transmission function of the spectrometer for the specific ith component. Therefore, a homogeneous distribution of the ith component over the probing depth is assumed. In present case, this assumption is not quite true, as discussed in the layer structure model below. Therefore, the resulting concentration should only be taken as qualitative guide. The relationship

$$T_i \propto \left(\frac{E_{\text{kinetic}}}{E_{\text{pass}}}\right)^{-1} \tag{2}$$

is used, as previously reported,[26] where E_{kinetic} is the kinetic energy of photoelectrons, E_{pass} is the pass energy of the spectrometer.

Table I presents the atomic concentration ratios calculated for both surface-sensitive and bulk-sensitive measurements from both the SeS_2 as-treated and HCl-cleaned-only surfaces. An increase was seen in the As-to-Ga atomic concentration ratio for the as-treated surface with respect to the HCl-cleaned-only surface for both bulk-sensitive and surface-sensitive measurements. The Se-to-S atomic concentration ratio for the bulk-sensitive measurement is substantially larger than that for the surface-sensitive measurement. These results indicate that the surface composition changes in depth.

TABLE II. Parameters used in the deconvolution of As $3d$, Ga $3d$, Se $3d$, and S $2p$ photoemission spectra.

	As $3d$	Ga $3d$	Se $3d$	S $2p$
Spin orbit (eV)	0.72±0.03	0.45	0.86	1.15
Branching ratio	2/3	2/3	2/3	0.5
Gaussian width (eV)	0.33±0.02	0.33	0.38	0.5

3. Core-level studies

In order to further study the surface chemistry of the as-treated surface, Ga $3d$, As $3d$, Se $3d$, and S $2p$ core-level photoemission spectra were measured individually with high instrumental resolution from both the as-treated and thermally annealed surface. The combined energy resolution was less than 0.2 eV. The results from the as-treated surface are presented in this section. Spectral deconvolution was performed on the measured photoemission spectra using a spectral synthesis approach. The spectral line shape was simulated by a suitable combination of two single line shapes possessing a Gaussian broadening function. The spin-orbit splitting, branching ratio, and Gaussian width were assumed to be the same for all components of a given core level. During fitting process, variable parameters were energy positions and peak areas, with Gaussian width, spin-orbit splitting, and branching ratio treated as fixed parameters. The confidence level for the fitting results of energy position and peak areas is 95%. On physical grounds, the spin-orbit splitting, Gaussian width, and branching ratio do not change appreciably for different components of the same structure.[27] The branching ratio is always close to the theoretical values of 2/3 for the $3d$ core level, and 1/2 for the $2p$ core level. These parameters for Ga $3d$ and As $3d$ core-level spectra were determined from the Ga $3d$ and As $3d$ core-level spectra of the thermal-cleaned reference surface, and agree well with previous determinations.[23,28] The previously reported deconvolution parameters for Se $3d$ and S $2p$ were also used.[23,29,30] Table II lists the parameters used for the deconvolution of As $3d$, Ga $3d$, Se $3d$, and S $2p$ spectra. The experimental data are represented by dots and the solid line by the sum of the simulated components of identical line shape. The matching of the simulated curves to the experimental data in the wings was occasionally problematic, and was attributed to difficulties in the subtraction of the nonlinear background. While HCl precleaning process was employed in our experiment, no Cl peak was observed for both HCl-cleaned-only and as-treated samples.

The As $3d$ photoemission spectrum from the as-treated GaAs(100) surface is shown in Fig. 2. There are three shoulders in addition to the main As–Ga based peak. The first two peaks, which have chemical shifts from the As–Ga based peak of 2.5 and 1.43 eV, respectively, are ascribed to As–S based peaks and labeled as As–S (1) and As–S (2), respectively. A third peak having a chemical shift of 0.86 eV is assigned to the As–Se peak. The chemical shifts of these peaks, from the As–Ga reference peak, are very close to previously reported values.[23,29,30]

The Ga $3d$ spectrum from the as-treated surface is shown in Fig. 3. A clear shoulder peak is observed at 1.0 eV

Downloaded 29 Dec 2006 to 128.104.198.71. Redistribution subject to AIP license or copyright, see http://jap.aip.org/jap/copyright.jsp

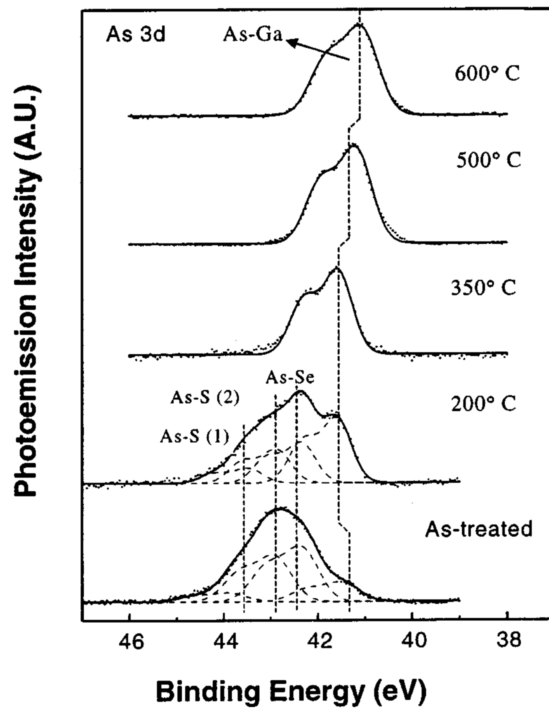

FIG. 2. As 3*d* core-level photoemission spectra from the as-treated GaAs(100) surface and changes induced in the core levels as a function of thermal annealing at (a) 200 °C, (b) 350 °C, (c) 500 °C, and (d) 600 °C. The dotted lines are used to indicate the chemical shift of individual core-level peak due to the progressive desorption of the SeS_2 passivating layer as a result of thermal annealing. This chemical shift can be attributed to the shift of surface Fermi level resulting from the change of surface chemistry due to thermal annealing. The disappearance of the As–S based and As–Se based peaks by thermal annealing under 350 °C indicates the low stability of As–S and As–Se based bonds. (Photon energy=88 eV in all cases.)

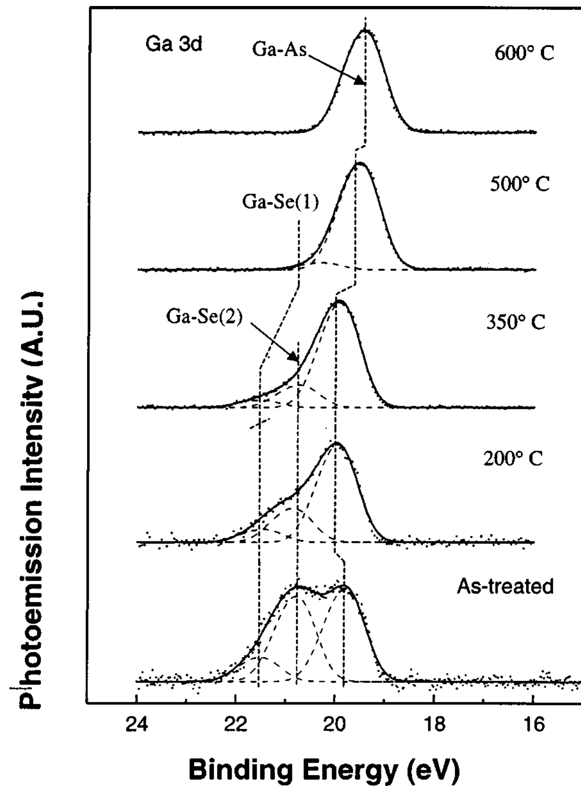

FIG. 3. Ga 3*d* core-level photoemission spectra from the as-treated GaAs(100) surface and the changes induced in the core levels as a function of annealing at (a) 200 °C, (b) 350 °C, (c) 500 °C, and (d) 600 °C. The disappearance of the Ga–Se (2) based peak coincides with an dramatic increase of band bending, indicating that the chemical bonding related to the Ga–Se (2) is the principal factor in the reduced band bending at the as-treated surface. (Photon energy=65 eV in all cases.)

higher binding energy than the main Ga-As peak. There is also a smaller shoulder at 1.7 eV higher binding energy from Ga–As peak. From the S 2*p* spectra presented later, there are no observed Ga–S based peaks. These peaks are therefore ascribed to Ga–Se bonds and labeled as Ga–Se (1) and Ga–Se (2), respectively. This assignment is also supported by the fact that the components ascribed to Ga–Se based bonds still remain after the complete desorption of S atoms during thermal annealing at 350 °C. Ga–Se (2) bonds are assumed to be Ga_2Se_3-like,[23] and Ga–Se (1) bonds are assumed to be the bonding states corresponding to $GaSe_x$ ($x > 1.5$)-like bonds. In a comparison to the Ga_2Se_3-like bonds, more charge transfer from Ga to Se per unit atom cause a bigger chemical shift for $GaSe_x$ ($x > 1.5$)-like bonds.

Figure 4 presents the Se 3*d* photoemission spectrum from the as-treated surface. Three peaks are observed. Separate measurements on thick SeS_2 layers on the GaAs, formed by evaporating SeS_2 solution on GaAs surfaces, rule out the possibility of Se–S bonds given the calculated binding energy for the Se–S bonds. The peak with highest binding energy is assigned to the Se–As bonds. The other two peaks are ascribed to the Se–Ga bonds. The amount of charge transfer from Ga to Se is considered to be larger than that from As to Se since the electronegativity difference between Ga and Se is larger than that between As and Se. Therefore, these peaks correspond to Se–As, Se–Ga (1), and Se–Ga (2)

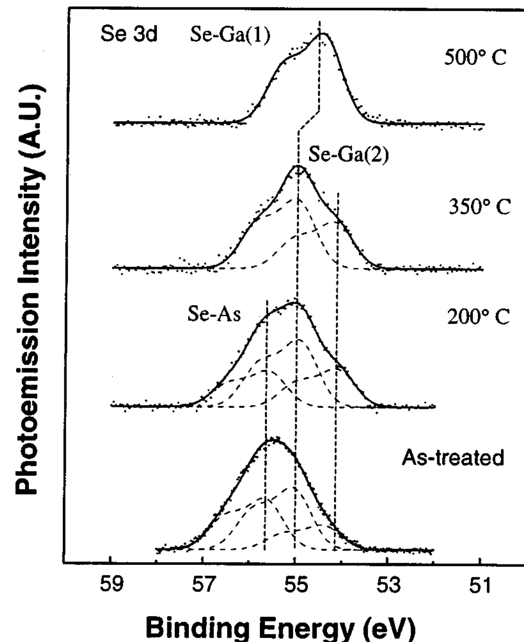

FIG. 4. Se 3*d* core-level photoemission spectra from the as-treated GaAs(100) surface and the changes induced in the core levels as a function of annealing at (a) 200 °C, (b) 350 °C, (c) 500 °C. Se–Ga based peaks dominate the Se 3*d* spectra. (Photon energy=100 eV in all cases.)

Downloaded 29 Dec 2006 to 128.104.198.71. Redistribution subject to AIP license or copyright, see http://jap.aip.org/jap/copyright.jsp

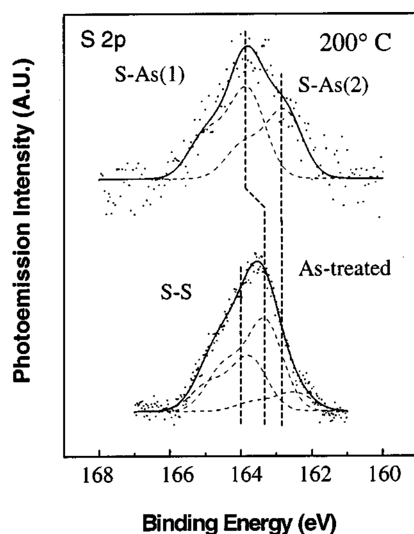

FIG. 5. S $2p$ core-level photoemission spectra of the as-treated GaAs(100) surface and changes induced in the core levels by thermal annealing at 200 °C. The S $2p$ signal drops below the detection limit after thermal annealing at 350 °C. (Photon energy=209 eV in both cases.)

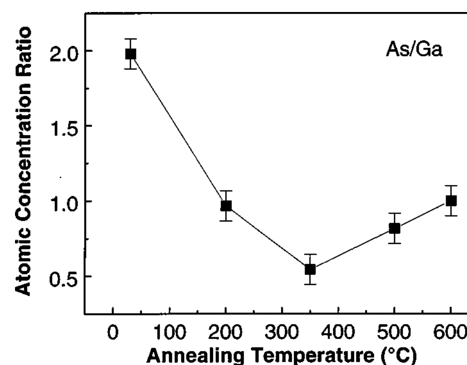

FIG. 6. As-to-Ga atomic concentration ratio as a function of the annealing temperature. The dramatic change of As-to-Ga atomic concentration ratio is observed during thermal annealing, suggesting a nonstoichiometric distribution of As atoms and Ga atoms in the as-treated surface region. The reduction of As/Ga ratio is attributed to the progressive desorption of the passivating overlayer. (Photon energy=205 eV.)

bonds. The binding energies for these peaks are very close to the previously reported values.[29,30] The peak of Ga_2Se_3-like bonds should have a lower binding energy than that of $GaSe_x$ ($x>1.5$)-like bonds, since the amount of charge transfer from the Ga atoms per selenium atom is larger for Ga_2Se_3-like bonds than that of $GaSe_x$ ($x>1.5$)-like bonds. Therefore, Se–Ga (1) and Se–Ga (2) are assumed to be $GaSe_x$ ($x>1.5$)-like and Ga_2Se_3-like bonds respectively, as previously mentioned in Ga $3d$ spectrum.

Figure 5 shows the S $2p$ photoemission spectrum from the as-treated surface. The spectrum is composed of two peaks of lower binding energy ascribed to S–As and the highest kinetic energy peak ascribed to S–S bonds. The binding energy for the S–S peak (164 eV) is very close to the previously reported value.[31] The binding energy differences between S–S peak and the other two peaks are 0.81 and 1.26 eV, respectively. These peaks are not attributed to S–Ga based bonds since the magnitude of the chemical shifts from S–S reference peak for these other two peaks are smaller than expected for S–Ga bonds.[29] This assignment is in agreement with the results of Ga $3d$ spectrum from the as-treated surface, in which there is no Ga–S based peak noted.

B. Thermal annealing study

1. Atomic concentration ratios

The atomic concentration ratios of different elements changed dramatically during subsequent annealing at the temperature ranging from 200 to 600 °C. In order to monitor the evolution of the relative peak intensity ratios of different elements due to thermal annealing, a survey scan of all these core-level peaks was carried out at an incident photon energy of 205 eV before and after each annealing step. The progressive desorption of S and Se atoms, due to thermal annealing, was observed by measuring the intensity of the Se $3d$ and S $2p$ core-level peaks. The complete desorption of S atoms took place under relatively low temperature annealing conditions, while the Se $3d$ spectrum was still detectable up to an annealing temperature of 500 °C. Figure 6 presents the evolution of As-to-Ga atomic concentration ratio with progressive annealing. Low-temperature annealing reduced the As-to-Ga atomic concentration ratio, while the ratio increased with further high-temperature annealing. After complete desorption of both Se and S, this ratio approaches the stoichiometry of GaAs. The dramatic change in the As-to-Ga atomic concentration ratio, due to thermal annealing, also suggests a nonstoichiometric distribution of As atoms and Ga atoms at the as-treated surface.

2. Core-level studies

The evolution of As $3d$, Ga $3d$, Se $3d$, S $2p$ core-level spectra due to thermal annealing is presented in Figs. 2–5. The dotted lines are used to indicate the chemical shift of individual core-level peak due to the progressive desorption of the SeS_2 passivating overlayer as a result of thermal annealing. This chemical shift can be attributed to the shift of surface Fermi level resulting from the change of surface chemistry due to thermal annealing. The deconvolution method is same as in Sec. III A *3*. Figure 2 presents the evolution of As $3d$ spectra with progressive thermal annealing. After thermal annealing at 350 °C, the As $3d$ core-level spectra can be fit by a single peak. It is assumed that this peak is attributed to As–Ga bonds. This result indicates that both As–S based bonds and As–Se based bonds are eliminated by thermal annealing at 350 °C.

Figure 3 presents the evolution of Ga $3d$ spectra with progressive thermal annealing. The intensity of the Ga–Se based peaks was reduced, with respect to the intensity of Ga–As based peak, by thermal annealing. During thermal annealing under 350 °C, this can be attributed to the desorption of the uppermost surface layer which can increase the Ga–As based peak intensity. During thermal annealing above 350 °C, the reduction of Ga–Se based peak intensity is attributed to progressive desorption of Se atoms. Only one

Downloaded 29 Dec 2006 to 128.104.198.71. Redistribution subject to AIP license or copyright, see http://jap.aip.org/jap/copyright.jsp

Ga–Se based peak was observed after thermal annealing at 500 °C. This Ga–Se based peak is attributed to Ga–Se (1)-like bonds.

The evolution of the Se 3*d* spectra due to thermal annealing, presented in Fig. 4, is consistent with the corresponding evolution of both the As 3*d* and the Ga 3*d* spectra. In comparison to the as-treated surface, the intensity ratio of the Se–As based peak to the Se–Ga based peak decreased due to thermal annealing at 200 °C. The Se–As based peak disappeared during thermal annealing at 350 °C, which is consistent with the disappearance of the As–Se based peak in corresponding As 3*d* spectra. After thermal annealing at 500 °C, the peak associated with Se–Ga (1) remains. Progressive desorption of the passivating layer during thermal annealing results in the residual Se atoms in the uppermost surface layer being composed of a single chemical-bonding state. This bonding state is ascribed to $GaSe_x$ ($x>1.5$)-like bonds, as mentioned above, in which one Ga atom is bonded to more than one Se atom. The evolution of the S 2*p* spectra with thermal annealing is presented in Fig. 5. The S–S based peak was not observed after 200 °C annealing. The S 2*p* spectra became undetectable after thermal annealing at 350 °C, which is consistent with the disappearance of the As–S based peaks in the corresponding As 3*d* spectra.

3. The shift of surface Fermi level

The core-level study indicates that thermal annealing in UHV with increasing temperature can selectively break the chemical bonds on the SeS_2-treated GaAs(100) surface. The relationship between the chemical bonding on the surface and the position of the surface Fermi level was also determined in this study.

The position of surface Fermi level can be determined from the energy position of the Ga–As peaks in the core-level spectra. Generally, this is the most accurate means of determining the shifts in band bending since the core-level energies below the immediate surface are least affected by the surface chemistry.[27] The difference between the Ga 3*d* core-level binding energy and valence band maximum in bulk GaAs is 18.75 ± 0.03 eV.[32] Therefore, the following equation is used to determine the position of surface Fermi level:

$$E_F=E_{\mathrm{Ga}\,3d}-18.75\ \ \mathrm{eV}, \qquad (3)$$

where E_F is the surface Fermi level position relative to the valence band maximum and $E_{\mathrm{Ga}\,3d}$ is the observed Ga 3*d* core-level binding energy for Ga–As bonds. Averaging the data over multiple data sets gave the E_F position with a standard deviation $\sigma=0.01$ eV. Figure 7 presents the position of surface Fermi level for the as-treated surface and thermally annealed surface. The shift of the surface Fermi level within band gap was monitored under controlled thermal annealing conditions allowing for the determination of the specific chemical entities responsible for the movement of the surface Fermi level. During thermal annealing at 200 °C, the surface Fermi level moves toward conduction band. After thermal annealing at 350 °C, there is only As–Ga based peak left in the As 3*d* spectra, indicating that both As–S based and As–Se based chemical bonds are eliminated from the surface. The downward movement of surface Fermi level toward valence band is very small, which suggests that both As–S and As–Se based surface chemical bonds are not important in determining the surface Fermi level position. During thermal annealing at 500 °C, the shift of the surface Fermi level toward valence band is quite dramatic. A single peak remains in the Se 3*d* spectra after thermal annealing at 500 °C, indicating the loss of most of the surface Se atoms. This result is consistent with the corresponding Ga 3*d* spectra, in which one of Ga–Se based peaks disappears. The breaking of Ga–Se (2) based bonds by thermal annealing at 500 °C is correlated with the movement of the surface Fermi level toward the valence band, indicating that the chemical bonding corresponding to Ga_2Se_3-like bonds, is most likely responsible for the elimination of midgap states and the measured surface Fermi level position on the as-treated surface.

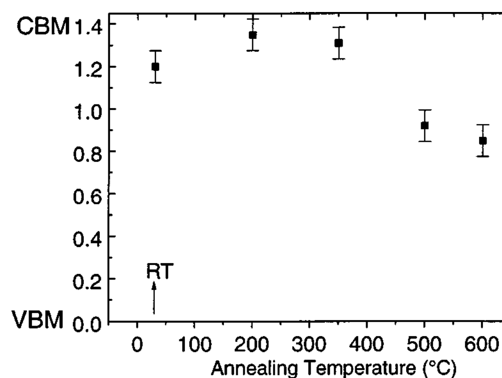

FIG. 7. Position of the surface Fermi level relative to the band edges as function of the annealing temperature for a highly *n*-doped GaAs(100). The shift of the surface Fermi level from the unpinned position near CBM toward midgap is due to the progressive desorption of the passivating overlayer.

IV. DISCUSSION

The SeS_2 treatment results in several effects that indicate the removal or redistribution of the midgap surface states. The enhancement in the PL intensity from both *n*- and *p*-GaAs(100) indicates that the GaAs(100) surface was electronically passivated with the reduction of surface recombination velocity and or surface charge density.[33] The experimental results from synchrotron radiation photoemission study of the SeS_2-treated GaAs(100) surface can be used to develop a consistent picture of the surface chemical structure and electronic properties underlying the passivation mechanism of the as-treated surface.

A. Surface chemistry of the SeS_2-treated GaAs(100) surface

The atomic concentration ratio study indicates that the as-treated surface consists of a chemically stratified structure at the surface. A structural layer model is proposed based on these experimental results. While other models are possible, the proposed model is both consistent with the experimental results found in the core-level and thermal annealing studies. A schematic diagram of the proposed structural layer model

Downloaded 29 Dec 2006 to 128.104.198.71. Redistribution subject to AIP license or copyright, see http://jap.aip.org/jap/copyright.jsp

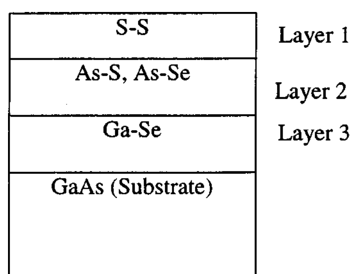

FIG. 8. Structural model for the passivated GaAs(100) surface. The Ga–Se layer (layer 3) provides the surface electronic passivation, and the S–S, As–S, As–Se (layer 1 and layer 2) protect the surface from interaction with the atmosphere or other chemical environments.

is shown in Fig. 8. The surface is terminated with S–S bonds (layer 1). The uppermost surface region is As rich (layer 2), while the adjacent region is As deficient (layer 3). The As atoms are bonded to both S atoms and Se atoms in the As-rich region. The As-deficient region consists primarily of Ga-based selenides. The layered structure of the as-treated surface can be attributed to the surface reactions between S, Se, As, and Ga atoms, such as an exchange reaction between Se atoms and As atoms.

Occurrence of an anion exchange reaction between Se and As atoms has also been identified for GaAs(100) treated with H_2Se [34] and by adsorption of Se atoms on GaAs surfaces.[29,30] The exact mechanism and kinetics of this exchange reaction are still unknown. The Pauling covalent radius of As (0.121 nm) is closer to that of Se than to any of the other chalcogenides. The covalent radii of S, Se, and Te are 0.104, 0.117, and 0.137 nm, respectively.[35] Furthermore, the bulk lattice constant for GaAs is 0.565 nm and those for the zinc-blende-structured Ga_2S_3, Ga_2Se_3, Ga_2Te_3 are listed as 0.518, 0.543, and 0.59 nm, respectively.[18] Structurally, Se atoms, as opposed to S or Te atoms, would most readily exchange with As atoms within the GaAs. In Fig. 4, it was observed that the peak intensity ratio of Se–As to Se–Ga (1) and Se–Ga (2) was decreased during thermal annealing at 200 °C. Some of Se atoms can form a Ga_2Se_3-like compound with Ga atoms at the surface, which corresponds to Ga–Se (2) in this study, and is correlated with the observed shift of the surface Fermi level on the as-treated surface. The Ga_2Se_3-like phase has also been suggested for the GaAs surface treated with H_2Se gas.[34]

In order to derive a quantitative model of the layered structure for the as-treated surface, the measured core-level photoemission peak intensity was analyzed using the standard layer-attenuation model.[36] The following assumptions were made: (a) There are no Ga atoms in both layer 1 and layer 2. (b) The ratio of Ga-to-Se in layer 3 is same as the ratio of Ga-to-As on the HCl-cleaned-only GaAs surface. The thickness of the layer 1 and layer 2 is estimated from the observed attenuation of Ga 3*d* peak of the as-treated surface relative to the HCl-cleaned-only surface. The intensity ratio of the Ga 3*d* ratio can be expressed in term of layer-attenuation model as

$$\frac{I_{\mathrm{Ga}}^1}{I_{\mathrm{Ga}}^2}=\frac{C_{\mathrm{beam}}^1}{C_{\mathrm{beam}}^2}\times\frac{E_{\mathrm{pass}}^1}{E_{\mathrm{pass}}^2}\times\exp\left(-\frac{d}{l}\right), \tag{4}$$

where I_{Ga} is the intensity of Ga 3*d* core-level peak, C_{beam} is the current of the synchrotron radiation beamline, E_{pass} is the pass energy of the CMA spectrometer, d is thickness of layers 1 and 2, and l is the photoelectron escape depth. Calculations result in a thickness, d, of ~0.54 nm, indicating that the thickness of the layer 1 and layer 2 is equivalent to several atomic layers. The proposed surface model accounts for the surface chemical compositional structure over several atomic layers. We also investigated the surface morphology after $SeSe_2$ treatment using atomic force microscopy (AFM). Our results indicate that the SeS_2-passivated GaAs(100) surface (scan size: 5 μm×5 μm) is relatively smooth and uniform. Compared to the HCl-cleaned-only surface, the SeS_2 treatment did not result in measurable change on surface morphology. While not conclusive, this smooth surface topology does not exhibit a substantial change in the surface structure between the SeS_2-treated and untreated samples. The passivation appears to conformal to the surface. Islanding of a small lateral extent may be missed by the AFM images. Previous workers in this field have reported ordered surfaces after SeS_2 passivation also indicating a smooth conformal reaction front during passivation.[37] In lieu of higher resolution measurements not available to the present study, we will work with the assumption of a smooth, conformal passivation surface.

Since most of As atoms are bound to S or Se atoms in the uppermost surface region, the intensity of As–Ga peak should be relatively small for As 3*d* spectra. The existence of the underlying As-deficient layer can also lead to a decrease of the intensity of As–Ga peak. After thermal annealing at 350 °C, the S 2*p* peak was no longer detected and As 3*d* spectra can be fit with a single peak corresponding to the As–Ga bonds. The line shape of Ga 3*d* spectra did not appreciably change during thermal annealing at 350 °C. All these results suggest that the S atoms are primarily bound to As atoms.

The progressive desorption of the passivating layer due to thermal annealing can be used to determine the stability of different chemical bonds. Only S–S bonds disappeared during thermal annealing at 200 °C as well as the high volatility of element sulfur, suggesting that these bonds are least stable under these thermal annealing conditions. An increased annealing temperature of 350 °C results in the disappearance of S 2*p* spectra. The diminution of the S 2*p* peak coincided with the disappearance of As–S (1) and As–S (2) peaks in As 3*d* spectrum. The As–Se based peak in the Se 3*d* spectra also disappeared during thermal annealing at 350 °C. The Se 3*d* spectrum was subsequently fit with only two components ascribed to Ga–Se based peaks. These annealing results indicate that both As–S bonds and As–Se bonds are not as stable as the Ga–Se bonds under these thermal annealing conditions. The Ga–Se based peaks were detectable up to 500 °C, indicating that these bonds are the most stable bonds.

B. Surface passivation mechanisms

GaAs surface Fermi level pinning has been an important subject in both the surface science and semiconductor device

Downloaded 29 Dec 2006 to 128.104.198.71. Redistribution subject to AIP license or copyright, see http://jap.aip.org/jap/copyright.jsp

fabrication. The mechanism underlying Fermi level pinning is specific to the surface structure, orientation and chemistry.[38–41] An end goal of the chemical treatment of the GaAs surface is to reduce the GaAs surface state density, as well as to control the GaAs surface Fermi level position. The surface chemical environment determines the surface recombination velocity and the type and density of surface states. In this study, the reduced band bending for the as-treated surface, with respect the HCl-cleaned-only surface, is attributed to the formation of Ga–Se bonds during the SeS_2 treatment.

The passivation effect of chalcogen atoms (S, Se, and Te) for GaAs surfaces has triggered extensive theoretical studies of the correlation between surface electronic properties and chemical bonding on the GaAs surface.[42–44] Pseudopotential calculations for the S–GaAs system have shown that the electronic passivation could be due to the establishment of S–Ga chemical bonds, for which the bonding and the antibonding levels are found to lie out of the forbidden gap. This is contrast to S–As chemical bonds, which do not reduce the surface state density within the gap.[44] The first-principle pseudopotential calculation of the GaAs(100) surfaces, adsorbed with a monolayer of chalcogen atoms (S, Se, and Te), predicts that the chalcogen atoms adsorb at the bridge site on both Ga-terminated and As-terminated GaAs surfaces and form covalent bonds with Ga and As atoms.[42] The chalcogen–Ga bond is found to be stronger than the chalcogen–As bond. Chalcogen–Ga bonds, in general, also greatly reduce the surface state density in GaAs midgap region, while the chalcogen–As bonds do not. Such chalcogen–Ga bonds are dominant on the chalcogen-treated GaAs surface and are responsible for the passivation of the surface. The results of our study are consistent with these theoretical observations. The present analysis shows that a thin selenide layer of Ga_2Se_3-like bonds is formed adjacent to the bulk GaAs substrate that is principally responsible for the observed surface electronic passivation.

A methodology for passivating compound semiconductors has been suggested in which two overlayers are employed.[45] The first layer electrically defines the surface and the second or uppermost layer provides long-term protection against reaction with the ambient. For the SeS_2-treated GaAs(100) surface, this type of layered surface structure is naturally formed. The thin Ga-based selenide layer below the surface provides the requisite chemical bonding that improves the electronic properties of the surface, while the S atoms adsorbed on the surface and the adjacent As-rich region may serve to protect the underlying passivating layer from the atmosphere or other chemical environments. The long-term stability of the SeS_2-treated GaAs(100) surface has been investigated in our lab by photoreflectance measurements using the techniques described by Geisz *et al.*[46] Our results indicated that the SeS_2-treated GaAs(100) surface was stable over several months with negligible shift in the surface Fermi level being noted. These results will be published elsewhere.[47]

V. CONCLUSION

The SeS_2-treated GaAs(100) surfaces have been systematically studied with synchrotron radiation photoemission spectroscopy. The combined core-level peak intensity ratio and core-level spectra studies have been used to develop a structural model in which the SeS_2-treated surface consists of a chemically stratified structure over a few atomic layers below the surface. The as-treated surface is terminated with S–S bonds. The uppermost layer is As rich, in which As atoms are bonded to the S atoms and Se atoms. One layer adjacent to the bulk GaAs consists of Ga-based selenides and is associated with the unpinning of the surface Fermi level on the as-treated surfaces. This layered structure is shown to both provide surface electronic passivation and protect the surface from subsequent interaction with the ambient.

ACKNOWLEDGMENTS

This work was supported by NSF under Award No. CTS-9510099. It is based upon research conducted at the Synchrotron Radiation Center, University of Wisconsin-Madison, which is supported by the NSF under Award No. DMR-9531009. Facility support of the NSF Materials Research Science and Engineering Center on Nanostructured Materials and Interfaces is gratefully acknowledged.

[1] J. A. Van Vechten, Corros. Sci. **31**, 39 (1990).
[2] D. S. L. Mui, H. Liaw, A. L. Demirel, S. Strite, and H. Morkoc, Appl. Phys. Lett. **59**, 2847 (1991).
[3] Q. D. Qian, J. Qiu, M. R. Melloch, J. A. Cooper, Jr., L. A. Kolodziejski, M. Kobayashi, and R. L. Gunshor, Appl. Phys. Lett. **54**, 1359 (1989).
[4] J. Lgowaski, M. Kaminska, J. M. Parsey, Jr., H. C. Gatos, and M. Lichtensteiger, Appl. Phys. Lett. **4**, 1078 (1982).
[5] J. C. Nabity, M. Stavola, J. Lopata, W. C. Dautremont-Smith, C. W. Tu, and S. J. Pearton, Appl. Phys. Lett. **50**, 921 (1987).
[6] F. Capasso and G. F. Williams, J. Electrochem. Soc. **129**, 821 (1982).
[7] M. S. Carpenter, M. R. Melloch, and T. E. Dungan, Appl. Phys. Lett. **53**, 66 (1988).
[8] M. S. Carpenter, M. R. Melloch, M. S. Lundstrom, and S. P. Tobin, Appl. Phys. Lett. **52**, 2157 (1988).
[9] C. J. Sandroff, R. N. Nottenburg, J.-C. Bischoff, and R. Bhat, Appl. Phys. Lett. **51**, 33 (1987).
[10] J. R. Waldrop, Appl. Phys. Lett. **47**, 1301 (1985).
[11] D.-W. Tu and A. Kahn, J. Vac. Sci. Technol. A **3**, 922 (1985).
[12] B. J. Skromme, C. J. Sandroff, E. Yablonovitch, and T. Gmitter, Appl. Phys. Lett. **51**, 2022 (1987).
[13] Y. Wang, Y. Darici, and P. H. Holllway, J. Appl. Phys. **71**, 2746 (1992).
[14] R. S. Besser and C. R. Helms, Appl. Phys. Lett. **52**, 1707 (1988).
[15] X. Y. Hou, W. Z. Cai, Z. Q. He, P. H. Hao, Z. S. Li, X. M. Ding, and X. Wang, Appl. Phys. Lett. **60**, 2252 (1992).
[16] L. Ferrari, M. Fodonipi, M. Righini, and S. Selci, Surf. Sci. **331-333**, 447 (1995).
[17] S. A. Chambers and V. S. Sundaram, Appl. Phys. Lett. **57**, 2342 (1990).
[18] D. K. Biegelsen, R. D. Bringans, J. E. Northrup, and L. E. Swartz, Phys. Rev. B **49**, 5424 (1994).
[19] B. A. Kuruvilla, S. V. Ghaisas, A. Datta, S. Banerjee, and S. K. Kulkarni, J. Appl. Phys. **73**, 4384 (1993).
[20] S. Nozaki, S. Tamura, and K. Takahashi, J. Vac. Sci. Technol. B **13**, 297 (1995).
[21] B. A. Kuruvilla, A. Datta, G. S. Shekhawat, A. K. Sharma, P. D. Vyas, R. P. Gupta, and S. K. Kulkarni, Appl. Phys. Lett. **69**, 415 (1996).
[22] B. A. Kuruvilla, A. Datta, G. S. Shekhawat, A. K. Sharma, P. D. Vyas, R. P. Gupta, and S. K. Kulkarni, J. Appl. Phys. **80**, 6274 (1996).
[23] S. Takatani, T. Kikawa, and M. Nakazawa, Phys. Rev. B **45**, 8498 (1992).
[24] C. J. Spindt, R. S. Besser, R. Cao, K. Miyano, C. R. Helms, and W. E. Spicer, Appl. Phys. Lett. **54**, 1148 (1989).
[25] H. Sugahara, M. Oshima, H. Oigawa, and Y. Nannichi, J. Vac. Sci. Technol. A **11**, 52 (1993).

Downloaded 29 Dec 2006 to 128.104.198.71. Redistribution subject to AIP license or copyright, see http://jap.aip.org/jap/copyright.jsp

[26] J. Barth, F. Gerken, and C. Kunz, Nucl. Instrum. Methods Phys. Res. **208**, 797 (1983).
[27] G. Landgren, R. Ludeke, Y. Jugnet, J. F. Morar, and F. J. Himpsel, J. Vac. Sci. Technol. B **2**, 351 (1984).
[28] D. E. Eastman, T.-C. Chiang, P. Heimann, and F. J. Himpsel, Phys. Rev. Lett. **45**, 656 (1980).
[29] H. Sugahara and M. Oshima, H. Oigawa, H. Shigewa, and Y. Nannichi, J. Appl. Phys. **69**, 4349 (1991).
[30] T. Scimeca, Y. Watanabe, R. Berrigan, and M. Oshima, Phys. Rev. B **46**, 10201 (1992).
[31] S. Hüfner, *Photoelectron Spectroscopy*, 2nd ed. (Springer, Germany, 1996), p. 456.
[32] J. R. Waldrop, R. W. Grant, and E. A. Kraut, J. Vac. Sci. Technol. B **5**, 1209 (1987).
[33] H. Hasegawa, T. Saitoh, S. Konishi, H. Ishii, and H. Ohno, Jpn. J. Appl. Phys., Part 2 **27**, L2177 (1988).
[34] S. A. Chambers and V. S. Sundaram, Appl. Phys. Lett. **57**, 2342 (1990).
[35] L. Pauling, *The Nature of the Chemical Bond*, 3rd ed. (Cornell University Press, New York, 1960), p. 224.
[36] D. Biggs and M. P. Seah, *Practical Surface Analysis*, 2nd ed. (Wiley, New York, 1990), Vol. 1.
[37] B. A. Kuruvilla, A. Datta, G. S. Shekhawat, A. K. Sharma, P. D. Vyas, R. P. Gupta, and S. K. Kulkarni, J. Appl. Phys. **80**, 6274 (1996).
[38] W. E. Spicer, P. W. Chye, P. R. Skeath, C. Y. Su, and I. Lindau, J. Vac. Sci. Technol. **16**, 1422 (1979).
[39] W. E. Spicer, Z. Liliental-Weber, E. Weber, N. Newman, T. Kendelewicz, R. Cao, C. McCants, P. Mahowald, K. Miyano, and I. Lindau, J. Vac. Sci. Technol. B **6**, 1245 (1988).
[40] J. M. Woodall and J. L. Freeouf, J. Vac. Sci. Technol. **19**, 794 (1981).
[41] H. Hasegawa and H. Ohno, J. Vac. Sci. Technol. B **4**, 1130 (1986).
[42] T. Ohno, Surf. Sci. **255**, 229 (1991).
[43] S.-F. Ren and Y.-C. Chang, Phys. Rev. B **41**, 7705 (1990).
[44] T. Ohno and K. Shiraishi, Phys. Rev. B **42**, 11194 (1990).
[45] A. M. Green and W. E. Spicer, J. Vac. Sci. Technol. A **11**, 1061 (1993).
[46] J. F. Geisz, S. A. Safvi, and T. F. Kuech, J. Electrochem. Soc. **144**, 732 (1997).
[47] J. Sun, F. J. Himpsel, and T. F. Kuech, Mater. Res. Soc. Symp. Proc. **510**, 653 (1998).

Downloaded 29 Dec 2006 to 128.104.198.71. Redistribution subject to AIP license or copyright, see http://jap.aip.org/jap/copyright.jsp